JOURNAL OF COMPUTATIONAL PHYSICS **138,** 540–562 (1997)
ARTICLE NO. CP975833

Electrostatic Particle-in-Cell Simulation Technique for Quasineutral Plasma*

Glenn Joyce, Martin Lampe, Steven P. Slinker, and Wallace M. Manheimer

Plasma Physics Division, Naval Research Laboratory, Washington, DC 20375-5346
E-mail: joyce@ppd.nrl.navy.mil

Received October 7, 1996; revised August 29, 1997

We have developed a simulation method with *both* electrons and ions represented as particles-in-cell, in which the electrostatic field is determined from the requirement of quasineutrality rather than from Poisson's equation. This approach permits self-consistent calculation of the potential, in quasineutral situations where statistical fluctuations in the charge density frustrate the use of Poisson's equation. Time steps may be orders of magnitude longer than the plasma period, and mesh cells orders or magnitude longer than the Debye length, since electron plasma oscillations do not appear in the model and the Debye length is essentially set to zero. The simulation technique correctly represents kinetic features such as electron and ion Landau damping. The method is demonstrated by application to several simple test problems, including free expansion of a plasma, and linear and nonlinear ion sound. In the case of a plasma with strongly magnetized electrons, we apply the technique to determine the parallel electric field and parallel transport within the plasma. Quasineutral techniques for representing cross-field transport, and edge effects in bounded plasmas, will be discussed in subsequent publications.

Key Words: Quasineutral plasma; plasma simulation; particle simulation; particle-in-cell simulation.

1. INTRODUCTION

In particle-in-cell (PIC) simulations of plasmas, the standard technique [1–3] for calculating the electrostatic field is to solve Poisson's equation, with the charge density source term determined by the laydown of the densities of electrons and

* Supported by Office of Naval Research.

0021-9991/97 $25.00

ions, n_e and n_i. This procedure works well when the phenomena of interest proceed on time scales comparable to the electron plasma frequency ω_p and spatial scales comparable to the Debye length λ_D, and when there is substantial charge separation between electrons and ions. However, there are many plasma problems where the time and space scales are very much longer, and where the plasma maintains quasineutrality throughout, i.e., $|n_e - n_i| \ll n_i$. In these situations, it can be extraordinarily inefficient, or even unfeasible, to use Poisson's equation.

One problem is that the simulation supports electron plasma oscillations, and therefore the time step must be less than $2\omega_p^{-1}$ for stability. [4] In many situations, electron oscillations play no role in the phenomena of interest, and the shortest time scale that is actually of interest may be the period of a low-frequency wave, an ion time scale, a collisional time scale, or a time scale for electron transport over some macroscopic length. These time scales may be several orders of magnitude longer. Implicit algorithms [5–11] have often been used to avoid resolution of the electron plasma oscillation time scale. However, PIC simulation techniques also face a more fundamental difficulty arising from the circumstances of quasineutrality. The charge separation between electrons and ions, $n_e - n_i$, is often less than 10^{-5} of the density of either electrons or ions. If both electrons and ions are represented by simulation macroparticles, any attempt to calculate the potential directly from Poisson's equation would be futile, and overwhelmed by statistical noise. For example, in a million-particle 2D simulation with a 100×100 grid, there are typically 100 macroparticle electrons or ions in each cell. The physically correct value of the difference between the number of electrons and ions in the cell would be on the order of 10^{-3} macroparticles, clearly unresolvable. The statistical fluctuations within the cell, although typically less than the shot noise of $\sqrt{100}$ macroparticles, would typically be several orders of magnitude larger than the actual value of $n_e - n_i$. Numerical schemes involving Poisson's equation are obviously very difficult (and actually inappropriate) in the quasineutral limit. Indeed, Chen [12] noted long ago that, "In a plasma, it is usually possible to assume $n_e = n_i$ and $\nabla \cdot \mathbf{E} \neq 0$ at the same time. This is a fundamental trait of plasmas, one which is difficult for the novice to understand. *Do not use Poisson's equation to obtain E unless it is unavoidable!*"

Over the years, this advice has been applied in many analytic and numerical models which represent the plasma as a fluid, or represent the electrons as either a dielectric medium or a fluid within some hybrid scheme [13–22]. In cases where the electron inertia is neglected, these methods circumvent the use of Poisson's equation by determining $\mathbf{E}$ from the electron momentum conservation equation. In more complex treatments, electron inertia is retained, and the electric field is determined from the electron and ion continuity and momentum equations, together with the quasineutrality relation. These approaches, which are reviewed in detail by Hewett [22], have also been combined with simplified treatments of the electromagnetic equations. In these fluid–electron models, n_e and the irrotational part of the electron current J_e are not calculated from the response to specified fields, but rather are set to the magnitude necessary to preserve quasineutrality. This procedure eliminates temporal scales on the order of the electron plasma frequency, as well as spatial structures on the Debye length scale.

Hybrid models of this type are the technique of choice for quasineutral plasmas whenever a fluid–electron formulation is acceptable. However, there are many situations in which a fluid representation of the electrons is simply not valid. For example, electron and ion kinetic phenomena may both be essential in modeling wave phenomena, or the self-consistent calculation of non-Maxwellian energy distributions may be essential to the modeling of inelastic collisional phenomena, e.g., ionization. In these types of situations, it may be necessary to resort to a PIC representation for both the electrons and ions, even though any such model will run considerably slower than a hybrid model. However, in PIC–electron/PIC–ion simulations, the electron density must be calculated by pushing particle electrons in response to fields, and no method has hitherto been available for doing this in a way that maintains quasineutrality.

We present here a new approach to the simulation of quasineutral plasmas with particle electrons and particle ions. Our approach is motivated by the quasineutral fluid techniques described in the previous paragraph, and our objective is to use grid spacing wide compared to the Debye length, and time steps long compared to the electron plasma frequency. We believe that the technique can be used to treat a wide variety of plasma problems. However, the primary objective of our present work is multi-dimensional overall modeling of an electron cyclotron resonance (ECR) reactor used for plasma processing. The plasma in this case is bounded, partially ionized, collisional, and magnetized, with a typical plasma density 10^{12} cm^{-3}, electron temperature several eV, and neutral density several times 10^{13}. The scale size of the reactor is tens of cm ($>10^3$ λ_D), and the time scales of interest range from 10 ns (electron transit times over cm size features, and electron collision times) to hundreds of μs (chemical equilibration), while $\omega_p^{-1} \cong 10^{-11}$ sec. In recent years, there has been considerable interest in the use of particle-in-cell/Monte Carlo (PIC/MC) codes to model this type of plasma [23–32]. Like pure PIC codes, these have typically used Poisson's equation to determine the electric field. In the present paper, we discuss only the method for determining the internal electric field within an unmagnetized bulk plasma, or parallel to the magnetic field in a magnetized bulk plasma. In subsequent publications [33–35], we shall discuss self-consistent techniques for dealing with sheaths, collisions, and chemistry, and with cross-field transport in a magnetized plasma, within a multi-dimensional quasineutral framework.

2. CALCULATION OF THE ELECTRIC FIELD

A. *Unmagnetized One-Dimensional Plasma*

We consider here only electrostatic fields, and for simplicity, we consider a one-dimensional system specified by Cartesian coordinate z, although the formalism can be extended to electromagnetic and multi-dimensional systems. We assume that the simulation is globally quasineutral, i.e., the total number of electrons is equal to the total number of ions. We also assume that the electron Debye length is small compared to any scale length resolved in the model, and the electron plasma frequency is fast compared to any time scale resolved in the model. Thus, if there

were any departure from local quasineutrality, the resulting strong electric field would drive electron currents to restore quasineutrality within a time scale of several electron plasma periods, i.e., essentially instantaneously compared to the time scales resolved in the model. Thus, the electric field always takes the value necessary to keep the electron density n_e equal to the ion density n_i. To specify this electric field, we can begin with the electron momentum conservation equation,

$$-eE = \frac{1}{n_e}\frac{\partial P_e}{\partial z} + \nu_e m_e u_e + \frac{1}{n_e}\frac{\partial}{\partial t}(n_e m_e u_e). \tag{1}$$

Here, $P_e(z, t)$ is defined as the electron kinetic pressure (including the stress associated with flow terms), $u_e(z, t)$ is the electron fluid velocity, and $\nu_e(z, t)$ is the mean electron momentum transfer collision frequency. These quantities can be specified as integrals over the electron distribution function $f_e(z, v, t)$,

$$P_e(z, t) \equiv \int dv\, m_e v^2 f_e(z, v, t), \tag{2a}$$

$$n_e u_e(z, t) \equiv \int dv\, v f_e(z, v, t), \tag{2b}$$

$$n_e \nu_e(z, t) \equiv \int dv\, \nu(z, v, t) f_e(z, v, t). \tag{2c}$$

These integrals, which appear in the first two terms on the right-hand side of Eq. (1), can be evaluated at each point of the grid, by laying down the mean quantities for the electrons assigned to that grid point. [The collision frequency $\nu(z, v, t)$ represents a sum over the various collisional processes which are represented in the simulation as Monte Carlo events, dynamical friction, etc.]

The first two terms on the right-hand side of (1) represent the ambipolar electric field, which balances the electron pressure gradients, flow gradients, and frictional forces. For low-frequency plasma processes which maintain quasineutrality (the only type of processes we wish to follow), the inertial term (last term of Eq. (1)) is smaller by order m_e/m_i. In a quasineutral *fluid* formulation, the inertial term would be neglected, and the ambipolar field would be used in the ion dynamical equations to calculate n_i at the next time step. Then n_e would simply be set equal to n_i. However, this is not quite sufficient in a particle simulation, where the electrons and ions evolve separately during each time step. With E set equal to the ambipolar field, $n_e(z, t)$ remains constant in time (except for statistical fluctuations), while the ion density $n_i(z, t)$ gradually evolves because of the relatively slow ion motion. Thus the ambipolar field alone will not maintain the quasineutrality relation

$$n_e(z, t) = n_i(z, t). \tag{3}$$

Even worse, particle simulations are always subject to statistical fluctuations in the density and flux of any species at any given grid point, typically limited to $\lesssim \sqrt{N}$, where N is the number of particles in a grid site. Thus, a particle simulation code must contain some mechanism for stably maintaining the quasineutrality relation (3) in the face of these fluctuations, which are of much larger order than m_e/m_i.

We have found that for low-frequency phenomena the kinetic information of interest is essentially contained in the ambipolar field, and that the last term of (1) serves only the functional purpose of keeping n_e equal to n_i. This opens up the possibility of keeping the ambipolar field but using an approximate technique to maintain Eq. (3), rather than calculating the actual inertial term. In earlier work [33], we have experimented with the technique of pushing the both the electrons and ions in the ambipolar field alone, and then applying an approximate correction field to the electrons which restores the quasineutrality condition. This worked well, and we were able to prove that kinetic properties such as the Landau damping of ion sound waves were preserved. However, this approach can become somewhat complicated, especially when care is taken to conserve energy exactly. In the present paper, we describe an approach which is even simpler, works extremely well over very long times, and has excellent stability and energy conservation properties. This approach is simply to replace Eq. (1) with a modified form of the ambipolar field,

$$-eE = \frac{1}{n_i}\frac{\partial}{\partial z}(n_i T_e) + \nu_e m_e u_e, \tag{4}$$

where the electron kinetic pressure $P_e(z, t) \equiv n_e(z, t)T_e(z, t)$ is replaced by $n_i(z, t)T_e(z, t)$, using the *ion* density instead of n_e. Here, T_e is a kinetic temperature (including the energy associated with flows), defined by

$$n_e(z, t)T_e(z, t) \equiv \int d\mathbf{v}\, m_e v^2 f_e(z, v, t). \tag{5}$$

This simple artifice causes the electron density to remain closely coupled to the ion density. This can be seen by writing the electron momentum conservation equation in the form

$$m_e\frac{\partial u_e}{\partial t} + \frac{1}{n_e}\frac{\partial}{\partial z}(n_e T_e) + eE + \nu_e m_e u_e = 0. \tag{6}$$

Using Eq. (4) for E, this gives

$$m_e\frac{\partial u_e}{\partial t} = T_e\frac{\partial}{\partial z}\ln\left(\frac{n_i}{n_e}\right). \tag{7}$$

Equation (7) shows that the electrons are always accelerated up the gradient of n_i/n_e, i.e., toward the point of maximum positive charge density. The result is that the electron density oscillates about the ion density. Although these oscillations are unphysical, they are rapid compared to ion time scales (but slow compared to electron plasma time scales), and the oscillation amplitude always remains small if the system is started in a quasineutral state and the time step is small enough to resolve the oscillation frequency. The stability properties of these oscillations will be discussed in Section 3, and examples will be given in Sections 5 and 6.

B. *Strongly Magnetized Electrons*

In the application which we are studying, ECR plasma sources, the electrons are strongly magnetized, with gyrofrequencies comparable to ω_p and gyroradii comparable to the Debye length. Since we do not wish to resolve these short time and space scales, it is convenient to use a guiding center representation of the electrons. An electron is characterized by its curvilinear coordinate ζ along the field line, its parallel velocity $v_\parallel \equiv d\zeta/dt$, and the magnitude $v_\perp$ of its perpendicular velocity. However, in practice it is more convenient to use the electron's magnetic moment $\mu \equiv m_e v_\perp^2/2B$ as the independent variable, rather than $v_\perp$, since μ is an adiabatic invarient. Here, B is the magnitude of the magnetic field. The equation of motion for an electron, between collisions, includes a mirror force term and is

$$\frac{dv_\parallel}{dt} = -eE_\parallel - \mu \frac{\partial B}{\partial \zeta}. \tag{8}$$

Within our quasineutral formulation, the electric field component parallel to **B** is then specified by the electron momentum equation in the form

$$-eE_\parallel = \frac{B}{n_e}\frac{\partial}{\partial \zeta}\frac{P_{e\parallel}}{|B|} + \overline{\mu}\frac{\partial B}{\partial \zeta} + \nu_e m_e u_{e\parallel} + \frac{1}{n_e}\frac{\partial}{\partial t}(n_e m_e u_{e\parallel}), \tag{9}$$

where $P_{e\parallel}$ and $P_{e\perp}$ are the electron kinetic pressure parallel and perpendicular to **B**, and $\overline{\mu} \equiv T_{e\perp}/B$ is the mean magnetic moment for electrons at a given location. [Note that the mirror force vanishes from Eq. (9) if $P_{e\parallel} = P_{e\perp}$.] As in the previous section, we simply drop the inertial term in (9) and replace $P_{e\parallel}$ by $n_i T_e$, so that $E_\parallel$ is specified by the equation

$$-eE_\parallel = \frac{B}{n_i}\frac{\partial}{\partial \zeta}\frac{n_i T_{e\parallel}}{|B|} + \overline{\mu}\frac{\partial B}{\partial \zeta} + \nu_e m_e u_{e\parallel}. \tag{10}$$

The determination of the transverse electric field $E_\perp$ involves the ion dynamics and, in the case of a bounded plasma in a conducting vessel, also couples to the sheath potentials. This will be discussed in a subsequent publication [35].

3. FORMAL ANALYSIS OF MODE STRUCTURE AND STABILITY

A. *Linearized Normal Modes*

To elucidate the way in which the electric field from Eq. (4) or Eq. (10) couples the electron and ion densities, we shall examine the linear normal modes supported by the system. Assuming an equilibrium with uniform density n_0 and temperature T_0, linearizing Eq. (4), assuming normal modes of the form $e^{i(kz-\omega t)}$, and neglecting collisions, we have

$$-eE = ikT_e + \frac{ikT_0}{n_0} n_i. \tag{11}$$

In the analysis of this section, we use linearized cold fluid equations for the ions, so that

$$n_{\mathrm{i}} = \frac{ikn_0eE}{\omega^2 m_{\mathrm{i}}}. \tag{12}$$

Combining Eqs. (11) and (12), we find

$$eE = -\frac{ikT_{\mathrm{e}}}{1 - k^2c_s^2/\omega^2}, \tag{13}$$

where $c_s^2 \equiv T_e/m_i$. To complete the analysis, we use the linearized Vlasov equation for the electrons,

$$\frac{\partial f_{\mathrm{e}}}{\partial t} + v\frac{\partial f_{\mathrm{e}}}{\partial z} - \frac{n_0eE}{m_{\mathrm{e}}}\frac{\partial F_0}{\partial v} = 0, \tag{14}$$

where $F_0(v)$ is the normalized equilibrium electron velocity distribution and $f_{\mathrm{e}}(z, v, t)$ is now the first-order perturbation. Using (13) in (14), we find

$$f_{\mathrm{e}} = -\frac{T_{\mathrm{e}}}{m_{\mathrm{e}}}\frac{1}{1 - k^2c_s^2/\omega^2}\frac{F_0'(v)}{v - \omega/k}. \tag{15}$$

T_{e} can be calculated by using

$$n_{\mathrm{e}} = \int dv\, f_{\mathrm{e}}(v) \tag{16}$$

and

$$n_{\mathrm{e}}T_0 + n_0T_{\mathrm{e}} = \int dv\, mv^2 f_{\mathrm{e}}(v). \tag{17}$$

Using (16) and (17) in (15) yields a dispersion relation

$$1 - \frac{k^2c_s^2}{\omega^2} + \int \frac{dv(v^2 - v_{\mathrm{e}}^2)F_0'(v)}{v - \omega/k} = 0. \tag{18}$$

We note first that if $c_s \to 0$, so that the ions are immobile, then

$$\omega = \pm kv_{\mathrm{e}}. \tag{19}$$

is a pair of exact solutions of Eq. (18). Here, $v_{\mathrm{e}} \equiv \sqrt{T_{\mathrm{e}}/m_{\mathrm{e}}}$ is the electron thermal velocity. This mode represents the unphysical high frequency oscillations that keep the electron density closely coupled to the ion density. However, the oscillation frequency ω is much smaller than ω_p. In a simulation with spatial grid scale Δz, the frequency is limited to $\omega < v_{\mathrm{e}}/\Delta z$, and if there is any spatial smoothing the highest-k modes are strongly damped, so that the highest meaningful frequency is actually much less. In a typical application such as our ECR simulations, Δz may

be about 1 cm, and $v_e/\Delta z$ of the order of 10^8 sec^{-1}, as compared to ω_p of order 10^{11} sec^{-1}.

We next examine the mode structure when $c_s \neq 0$. To perform the integrals simply in closed form, we assume that $F_0(v)$ is a Lorentzian distribution,

$$F_0(v) = \frac{1}{\pi} \frac{v_e}{v^2 + v_e^2}. \tag{20}$$

Then Eq. (18) becomes

$$1 - \frac{k^2 c_s^2}{\omega^2} = -\frac{2}{\pi} \int_{-\infty}^{\infty} \frac{dx\, x(1 - x^2)}{(1 + x^2)^2 (x - \Omega)}, \tag{21}$$

where $x \equiv v/v_e$ and $\Omega \equiv \omega/kv_e$. The contour for the integral in Eq. (21) can be closed above, and according to causality the pole at $x = \Omega$ is to be enclosed in the contour, even if Im Ω is negative. Using the method of residues, Eq. (21) reduces to

$$1 - \frac{m_e}{m_i} \frac{1}{\Omega^2} = 2 \frac{2\Omega^2 - i\Omega(1 - \Omega^2)}{(1 + \Omega^2)^2}. \tag{22}$$

If we multiply out the denominators in (22), we obtain a sixth-order polynomial equation,

$$\Omega^2(1 + \Omega^2)^2 - 4\Omega^4 + 2i\Omega^3(1 - \Omega^2) = \frac{m_e}{m_i}(1 + \Omega^2)^2. \tag{23}$$

We know that two of the roots lie at $\Omega = \pm 1$ if $m_e/m_i \to 0$. Assuming that these two roots lie close to ± 1, a perturbative solution gives

$$\omega = kv_e \left(\pm 1 + i \frac{m_e}{m_i} \right). \tag{24}$$

These modes are thus seen to be slightly unstable, by order m_e/m_i. However, this degree of instability is of no significance; the mode growth is so slow that it is obliterated by any of a number of incoherence effects that occur in all simulations. For example, we shall show in the next subsection that even the slightest degree of spatial smoothing damps the modes. As a practical matter, we can regard these as stable or damped modes that efficiently couple n_e to n_i to maintain quasineutrality.

Next, we look for low frequency modes with $|\Omega| \ll 1$. Keeping only lowest order in Ω in the real and imaginary terms of Eq. (23), we find one pair of low-frequency roots,

$$\omega = kc_s \left(\pm 1 - i \sqrt{\frac{m_e}{m_i}} \right). \tag{25}$$

These are the ion sound modes, with the correct dispersion relation in the limit $\lambda_D \to 0$, and with the correct representation of electron Landau damping for the Lorentzian distribution (20). We show in the Appendix that when a complete Vlasov treatment is used, the quasineutral model gives the correct results for both electron and ion Landau damping, and that the representation remains correct if there is electron–ion streaming.

The last two roots of the sixth-order equation (23) are a double root at $\Omega = i$. However, this is a spurious root, which is not a root of the original equation (22). Thus the formalism supports only two pairs of modes. One pair is the ion sound mode, correctly represented. The second pair of modes are the (unphysical, but essentially stable) high frequency modes which tightly couple n_e to n_i and thus preserve quasineutrality.

B. *Effect of Spatial Smoothing*

In practice, we find that it is necessary to apply some spatial smoothing to the electric field, as is often done in particle simulations [36], to overcome the fluctuations that are introduced by particle statistics and (in our case) are enhanced by the derivative operation in Eq. (4). One might wonder about the effect of smoothing on the stability of the scheme. Thus we reexamine the mode structure in the presence of smoothing.

The smoothed electric field $\tilde{E}$ may be represented as

$$\tilde{E}(z) = \int_{-\infty}^{\infty} dz'\, K(z - z')E(z'), \tag{26}$$

where $E(z)$ is given by

$$-eE(z) = \frac{\partial T_e}{\partial z} + \frac{T_0}{n_0}\frac{\partial n_i}{\partial z}, \tag{27}$$

and $K(z - z')$ is some symmetric kernel normalized to unity. Typically, $K(z - z')$ will be a smooth bell-shaped curve whose width at half-maximum, Δ, exceeds the cell size but is narrower than the wavelengths of primary interest. In Fourier representation, the convolution becomes simply

$$-e\tilde{E}_k = -eK_kE_k = ikK_kT_e + ikK_k\frac{T_0}{n_0}n_i. \tag{28}$$

Note that the Fourier transform K_k is always real, and $1 \geq |K_k|$ for all k. For long wavelengths where $k\Delta \ll 1$, the smoothing coefficient $K_k \to 1$ and the effect of smoothing is small but not zero. Using (28) in place of (11), we can retrace the derivation of the dispersion relation (22). We obtain the modified form

$$1 - K_k\frac{m_e}{m_i}\frac{1}{\Omega^2} = 2K_k\frac{2\Omega^2 - i\Omega(1 - \Omega^2)}{(1 + \Omega^2)^2}. \tag{29}$$

Equation (29) can be solved in the same way as (22). Again, there are four genuine roots. The two high-frequency modes which couple the electrons to the ions are now

$$\omega_k = kv_e \left[\pm\sqrt{(2 - K_k)K_k} - i\left(1 - K_k - \frac{m_e}{m_i}\right)\right]. \tag{30}$$

These modes are now seen to be damped as long as $1 - K_k > m_e/m_i$. Even the slightest degree of damping easily satisfies this condition for all modes. For example, if $K(z - z')$ is a Gaussian kernel with width Δ equal to two cells, then the Fourier transform kernel is $K_k = \exp(-k^2\,\Delta^2)$; short wavelengths are strongly damped, and all wavelengths out to 250 cells are at least weakly damped. In practice, we believe that the modes will be stable even if there is no formally applied smoothing; the smoothing effect of finite-size particles, and other standard numerical effects, will be sufficient to overcome the very slight degree of instability seen in Eq. (24). Thus, we conclude that the formula (4) for calculating the quasineutral field is indeed stable, and will cause the electrons to follow the ions in a quiescent fashion.

The two low-frequency solutions of (29) are

$$\omega_k = kc_s K_k^{1/2}\left(\pm 1 - iK_k^{3/2}\sqrt{\frac{m_e}{m_i}}\right). \tag{31}$$

Thus, as might be expected, the ion sound waves experience a reduction in frequency and in Landau damping, if there is smoothing on a scale comparable to the wavelength. Obviously, if one wishes to resolve sound waves of a given wavelength λ, the width of the smoothing kernel would be chosen to be considerably smaller than λ.

4. NUMERICAL IMPLEMENTATION

The choice of time steps is limited by a number of considerations, in addition to the obvious requirement that the time step resolve any time scale of interest, such as a wave period. (i) Accuracy requires that during a single time step, particles not traverse a range over which the electric field, or other macroscopic variables, change significantly. (ii) If collisions are an important aspect of the problem, and Monte Carlo methods are used to model them, the time steps for each species must also be limited to a fraction of the collision time. Both of these conditions typically allow the ion time step to be longer than the electron time step by a factor of the order of $(m_i/m_e)^{1/2}$. (iii) In addition, we have seen that Eq. (4) couples the electrons to the ions by inducing rapid stable electron oscillations with phase velocity equal to the electron thermal velocity v_e. Since these oscillations can be excited by statistical fluctuations in a single cell, a conservative procedure to avoid numerical difficulties is to choose the electron time step no larger than the cell size divided by v_e, and to recalculate the electric field acting on the electrons at each electron time step. In practice, this is a stronger restriction than is usually necessary. We have seen that the shortest wavelengths are strongly damped by smoothing effects. In addition, collisional situations are generally more forgiving, and typically allow further in-

creases in the time step. Thus, to summarize, we use relatively long ion time steps, chosen to satisfy conditions (i) and (ii), and subdivide these time steps, typically by a factor of the order of $(m_i/m_e)^{1/2}$, to obtain electron time steps that satisfy all three conditions. These conditions permit electron time steps that are typically three orders of magnitude larger than the time steps $\Delta t < 2/\omega_p$ that are needed for conventional PIC codes. The ion time steps are even larger, and in addition the spatial grid scales can be orders of magnitude larger than λ_D.

The electric field is calculated as a grid quantity at each electron time step, from Eq. (4), or Eq. (10) if the plasma is magnetized. This electric field is then applied directly to the electrons at each time step. To push the ions over a long ion time step, an electric field is used which is simply the average of the electric fields at each of the electron time steps during this ion time step. Thus there is significant temporal smoothing of Eq. (4) or (10), primarily a smoothing of the fluctuations in T_e, which helps to reduce statistical fluctuations in the ion motion.

The electrostatic potential energy of the plasma is $\int dV(n_i - n_e)e\phi$, and therefore is zero to the extent that exact quasineutrality is maintained. Thus, in the absence of inelastic scattering, the total kinetic energy should be conserved. This presumes, of course, that the electrons and ions see exactly the same electric field. However, energy conservation is preserved even if the electrons are pushed subject to the instantaneous electric field, and the ions to a time-averaged field, as long as the time averaging is properly centered over the ion time step. In practice, the oscillation of the electrons about the ion density profile means that quasineutrality is not exactly satisfied at any given time step, and long-term drifts in the total kinetic energy are possible. However, these are slight and very slow and can be controlled by maintaining a sufficient number of simulation particles and adequate spatial smoothing. Some examples will be given.

Because the electric field is calculated from the differential form (4), rather than an integral form such as Poisson's equation, it is necessary to use a rather large number of particles per cell to overcome statistical fluctuations. Furthermore, statistical problems arise first in low-density regions, where the denominator of the first term of Eq. (4) becomes small. In our 2D ECR simulation code, where there is significant electron collisionality, we get good results using an average of 100 particles per cell. Electron collisionality generally helps to smooth things out, and reduces the required number of particles. The collisionless examples studied in the next two sections are very severe test cases for the quasineutral method, and require an even larger number of particles to provide an excellent quantitative treatment. In the free expansion problem, the required number of particles is set by the low-density background, where we use 250 particles per cell. In the ion acoustic study, we simulate Landau damping and mode coupling as well as propagation of a small-amplitude wave (amplitude 5%); 2400 particles per cell are required to do this. However, we do not believe that this simulation could be done at all with any other fully PIC method.

We use a linear laydown for both the electrons and the ions. The ion density and the pressure are smoothed using standard filtering techniques [1]. The algorithm for pushing the particles is a centered difference scheme. The electrons are subcycled with typically 32 electron time steps for each ion time step. For the examples shown

here, the system is periodic, but in our ECR code the same method is used for a bounded system [35].

5. AN EXAMPLE: FREE EXPANSION OF A PLASMA

To illustrate the use of the quasineutral formulation, we consider a test problem which can be solved exactly, and also can be solved analytically within our formulation. Consider the free expansion of a plasma consisting of hot isothermal electrons and cold ions, beginning with a Gaussian spatial profile in one dimension:

$$f_i(z, v, 0) = \frac{1}{\sqrt{\pi} L_0} \exp\left(-\frac{z^2}{L_0^2}\right) \delta(v), \tag{32a}$$

$$f_e(z, v, 0) = \frac{1}{\sqrt{\pi} L_0} \sqrt{\frac{m_e}{2\pi T_{0e}}} \exp\left(-\frac{z^2}{L_0^2} - \frac{m_e v^2}{2T_{0e}}\right). \tag{32b}$$

Even though this is a problem that is easily solved analytically, it poses a stiff challenge to a a particle simulation, since there is a wide range in plasma density, and we assume there are no collisions. (Collisions make it much easier to implement this type of technique, by smoothing out statistical fluctuations.)

A. *Analytic Treatment: Exact Quasineutrality*

An exact solution to the Vlasov equation, with initial conditions specified by Eqs. (32), can be found in closed form. It corresponds to self-similar isothermal expansion,

$$f_i(z, v, t) = \frac{1}{\sqrt{\pi} L_i(t)} \exp\left(-\frac{z^2}{L_i^2(t)}\right) \delta\left(v - \frac{z\dot{L}_i(t)}{L_i(t)}\right), \tag{33a}$$

$$f_e(z, v, t) = \frac{1}{\sqrt{\pi} L_e(t)} \sqrt{\frac{m_e}{2\pi T_e(t)}} \exp\left[-\frac{z^2}{L_e^2(t)} - \frac{m_e}{2T_e(t)}\left(v - \frac{z\dot{L}_e(t)}{L_e(t)}\right)\right]. \tag{33b}$$

The expansion is driven by the electron pressure, with the ions dragged along by the electrostatic field. Thus a complete solution, using Poisson's equation, would show that $L_e(t)$ is larger than $L_i(t)$ by a small amount of the order of the Debye length. But to the extent that quasineutrality is observed, $L_e(t) = L_i(t)$, and $L_i(t)$ and $T_e(t)$ are determined by conservation of momentum and energy as the solutions to

$$\ddot{L}_i(t) = \frac{2T_e(t)}{m_i L_i(t)}, \tag{34a}$$

$$T_e(t) = T_e(0) - \frac{1}{2} m_i \dot{L}_i^2(t). \tag{34b}$$

Equations (34) can be solved for $L_i(t)$ in closed form. For the initial conditions specified by Eq. (32), the solution is

$$L_i(t) = \sqrt{L_0^2 + 2c_{s0}^2 t^2}. \tag{34c}$$

B. *Analytic Treatment Using Our Model*

Within our model, with E given by Eq. (4), it is easy to show that the electrons and ions each expand self-similarly, as in Eqs. (33), but with $L_e(t)$ not exactly equal to $L_i(t)$. $L_i(t)$ and $T_e(t)$ are given by Eqs. (34), but $L_e(t)$ is given by

$$\ddot{L}_e = 2v_e^2\left(\frac{1}{L_e} - \frac{L_e}{L_i^2}\right). \tag{35}$$

Rewriting Eq. (35) in terms of $\Delta \equiv (L_e - L_i)/L_i$, and subtracting (34a) from (35) gives

$$\ddot{\Delta} = -\frac{2v_e^2}{L_i^2}\left(\frac{(2+\Delta)\Delta}{1+\Delta} + \frac{m_e}{m_i}\right). \tag{36}$$

The first term of Eq. (36) causes Δ to oscillate about an equilibrium point. The second term causes a very small offset to the equilibrium point. (Interestingly, this offset is negative, so that in this formulation the ions lead the electrons by a displacement of order m_e/m_i.) Thus it is reasonable to assume $|\Delta| \ll 1$ and simplify (36) to

$$\ddot{\Delta} = -\left(\frac{2v_e(t)}{L_i(t)}\right)^2 \Delta. \tag{37}$$

Equation (37) indicates that Δ oscillates at the rapid frequency $\omega_0 = 2v_e/L_i(t)$, and since ω_0 is fast compared to the time scale for ion motion, these can be considered to be simple harmonic oscillations at a slowly varying frequency. These oscillations are not physical; they are the mechanism for coupling the electrons to the ions within our quasineutral formuation (4). However, they are stable oscillations which maintain a very small amplitude (in fact, comparable to the statistical fluctuations that would otherwise be present due to the finite number of particles), and thus are of no real significance. As mentioned earlier, a conservative condition for numerical stability is that the time step be less than ω_0^{-1}, and in fact, since statistical fluctuation can occur on length scales down to a single cell size Δz, less than $\Delta z/v_e$.

C. *Numerical Simulation*

Figures 1–3 show the results of a numerical simulation of the free expansion problem, for a hydrogen plasma ($m_i/m_e = 1836$). The system is initialized in accordance with Eq. (32), with $L_0 = 14$ cm and $T_e = 0.33$ eV. However, it was not possible in the simulation to allow the plasma to expand into a true vacuum, since the electric field from Eq. (4) depends on the reciprocal of the plasma density. (The noisy electric field in regions with very low density eventually dominates the problem.) In order to limit the noise, we added a low density floor (5% of the peak density) to the Gaussian density profile as can be seen in Fig. 1a. The system was made very long (400 cells) to avoid end effects, with the result that over half the

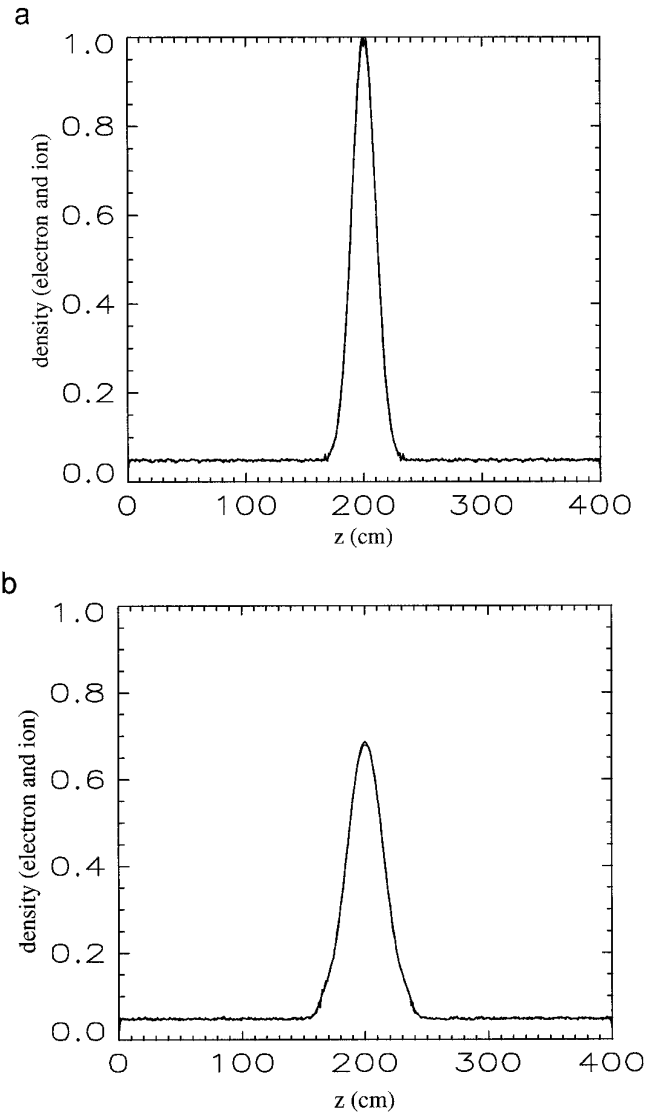

FIG. 1. (a) Initial conditions for the free expansion simulation: $n_e(z)$ and $n_i(z)$ at $t = 0$. (b) $n_e(z)$ and $n_i(z)$ at $t = 20$ μsec. In both cases, $n_e(z)$ and $n_i(z)$ are essentially indistinguishable.

simulation particles were in the background. In all, we used 200,000 macroparticle electrons and an equal number of ions. The cell size is $\Delta z = 1$ cm, and the time step is $\Delta t = 25$ ns.

Figure 1 shows the electron density profile (solid curve) and the ion density profile (dashed curve) at $t = 0$ and $t = 20$ μs. The deviations from quasineutrality are visible only at the peak density, and at the boundary with the low-density background plasma. We note that the expansion is very nearly self-similar, as predicted. (Eventually, small deviations from self-similarity, due to the presence of the low-density background, become visible.) Figure 2 shows $L_i(t)$ from the simula-

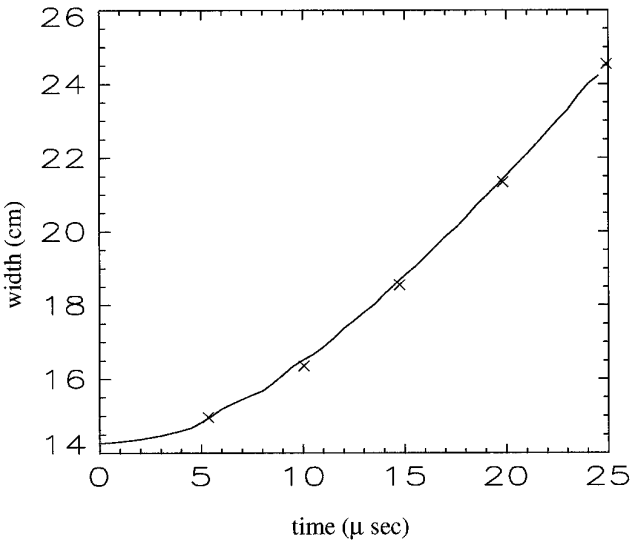

FIG. 2. Simulation result for expansion of the ion characteristic width $L_i(t)$. The x's are the analytic result (34c).

tion. The x's show the analytic solution (34c) for $L_i(t)$. We see that the expansion is smooth, and the analytic solution is well verified. Figure 3 shows plots of the total electron kinetic energy $W_e(t)$, the total ion kinetic energy $W_i(t)$, and the total kinetic energy $W(t)$. We note that the effect of the expansion is to convert the electron kinetic energy (which is nearly all thermal) to ion streaming energy. Overall kinetic energy is conserved to within 4%. To the extent that quasineutrality is

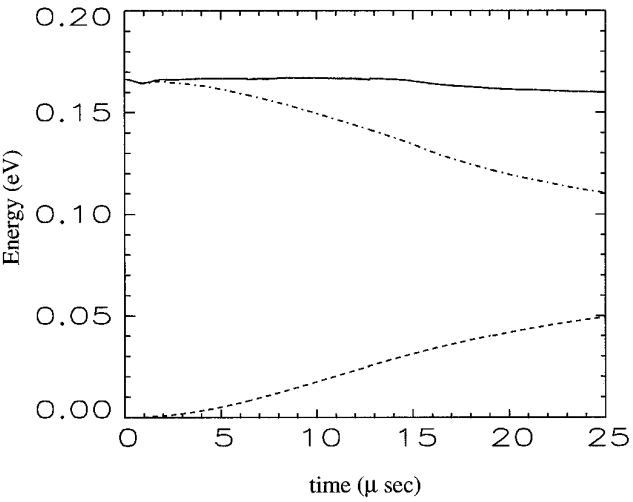

FIG. 3. Time dependence of the electron kinetic energy $W_e(t)$ (dot-dashed curve), ion kinetic energy $W_i(t)$ (dashed curve), and total kinetic energy $W(t)$ (solid curve) during free expansion.

maintained, there is essentially no potential energy, since the electron potential energy is always exactly the negative of the ion potential energy.

6. SECOND EXAMPLE: ION SOUND

Ion sound with wavelength much greater than λ_D is a simple example of a plasma mode that occurs on the ion time scale and maintains quasineutrality. It is therefore not an easy mode to simulate with a standard PIC code using Poisson's equation and a realistic value of m_e/m_i. In Section 3 above, we used a simplified model (Vlasov electrons with Lorentzian distribution, cold fluid ions) to show that the ion sound mode is contained within our quasineutral model, and in the Appendix we provide a full Vlasov analysis that shows that the quasineutral model gives exactly the correct dispersion relation, including electron and ion Landau damping terms. Here we show the results of simulations of ion sound within the nearly linear and nonlinear regimes, with the mass ratio $m_i/m_e = 1836$.

A. *Standing-Wave Ion Sound in the Linear Regime*

We initiate an ion sound standing wave by loading initial particle densities

$$n_e = n_i = n_0[1 + \alpha \sin(2\pi z/L)], \tag{38}$$

with the fluid velocities u_e and u_i initially zero for both species. The simulation is done with periodic boundary conditions in a 1D system of length $2L = 25$ cm, with cell length $\Delta z = 0.125$ cm; thus, there are two wavelengths within the box, and 100 cells per wavelength. The wave amplitude is taken to be $\alpha = 0.05$, and 2400 particles of each species are used, per cell. A very large number of particles is needed for this simulation to resolve the very small wave amplitude. The electron temperature is set to 1.33 eV, so that $v_e = 4.8 \times 10^7$ cm/sec, $c_s = 1.1 \times 10^6$ cm/sec, and the wave period should be $L/c_s = 11.3$ μs. The ions are initially cold. The ion time step is 15.6 ns, and the electrons are subcycled four times per ion time step.

The temporal evolution of the fundamental (wavelength L) Fourier mode of n_e and n_i is shown in Fig. 4. The densities are taken from the Fourier transforms of the instantaneous values of $n_e(z)$ and $n_i(z)$ at the ion time step. We see that the wave period is 11.1 μs, in excellent agreement with the theoretical value. We note that at any given time, quasineutrality ($n_e = n_i$) holds to better than 5%. Plots of the spatial dependence of the wave (not shown) indicate that the two wavelengths contained within the box are exactly the same.

Equation (A9) predicts Landau damping at the rate 9% per wave period. However, in a one-dimensional ion sound wave, even at wave amplitude $\alpha = 0.05$, trapping of the resonant electrons interferes with Landau damping at a very early stage. The trapping frequency is $\omega_T = \sqrt{keE/m_e}$, and according to the linearized version of Eq. (4), $E = k\alpha T_e$. Thus

$$\omega_T = kc_s\sqrt{\alpha\frac{m_i}{m_e}} = 9.6\,kc_s, \tag{39}$$

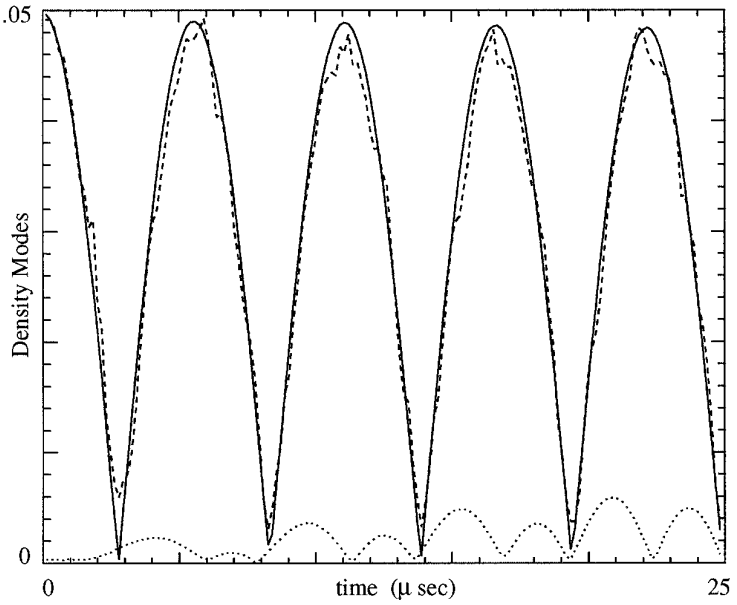

FIG. 4. Temporal evolution of the standing ion sound wave: electron density fundamental mode (solid curve), ion density fundamental mode (dashed curve), and electron density second harmonic mode (dotted curve). Each of the curves plots the absolute value of the wave amplitude.

and Landau damping should be over in a fraction of a wave period. The slight damping seen in Fig. 4 thus would seem to be the initial Landau damping, followed by a slower damping due to mode coupling to higher harmonics. The envelope of the second harmonic amplitude (wavelength $L/2$) grows to a level of 13% of the fundamental after two periods, as shown in Fig. 4. This is in excellent agreement with simple two-mode coupling theory, which predicts 15% at this time, and consequent damping of the fundamental by about 1.5%. From a computational point of view, we note that our grid resolution of 100 grid points per fundamental wavelength (i.e., 50 points per second harmonic wavelength) is necessary for a quantitatively accurate treatment of Landau damping and nonlinear processes in this very low-amplitude wave.

B. *Nonlinear Traveling Wave*

The nonlinear evolution of a standing wave is complex, but for traveling sound waves an analytic solution is possible via the method of characteristics [37]. Since λ_D is set to zero within our model, the ion sound waves are nondispersive, and therefore the mode coupling theory is essentially the same as that of ordinary sound waves in a neutral gas [37], with T_e playing the role of the gas temperature. (However, ion sound waves are isothermal, [38] whereas sound waves in a molecular gas are adiabatic. Therefore the adiabatic constant γ must be set to unity in the ion sound theory.) The velocity is found to be the solution of the implicit equation

$$u(z, t) = u(z - u(z, t)). \tag{40}$$

It is well known that Eq. (40) leads to steepening of the density and velocity profiles, and ultimately to wave breaking when $\partial u/\partial z$ becomes infinite. For an initial sinusoidal profile

$$\frac{u(z,0)}{c_s} = \alpha \sin\left(\frac{2\pi z}{L}\right); \tag{41}$$

this occurs when

$$t = t_{\text{break}} = \frac{L}{2\pi\alpha c_s}. \tag{42}$$

In Fig. 5 we show the results of a simulation similar to those of the previous subsection, except that the wave amplitude is larger at $\alpha = 0.20$ and a traveling wave is initiated by setting the initial ion fluid velocity as in Eq. (41). We note the steepening of the wave up to the point of breaking at about $t = 9$ μsec, in good agreement with the theoretical prediction $t = 9.04$ μsec. As the wave nears the breaking point, nonphysical structure such as the ripple and sharp peak in Fig. 5b begin to appear. These features appear to be associated with finite spatial resolution, and limit the accuracy of determination of the breaking point by perhaps 1 μsec. After wave breaking, the quasineutral theory is no longer correct, since λ_D length scales are relevant to the subsequent evolution of the ion acoustic shocks.

7. CONCLUSIONS

We have presented a method for doing plasma simulations with particle electrons and particle ions, in the quasineutral limit. The method permits (indeed, it requires) the use of grid spacing long compared to λ_D and time stepping long compared to ω_p^{-1}. We have demonstrated analytically that the method is stable (at least on a continuous time basis), and that it gives the correct dispersion relation for ion sound, including Landau resonance terms. We have also demonstrated the use of the method to simulate free expansion of a plasma, and linear and nonlinear ion sound.

We believe that the technique presented here should be useful for a variety of problems involving quasineutral plasmas. We are using this method in a 2D simulation code for magnetized plasmas, which includes in addition cross-field transport, sheaths at insulating or conducting walls, ECR heating, and collisions and chemistry. The techniques used to model these other aspects of the physics will be discussed in [35] and subsequent publications. The code runs for very long times (hundreds of μsec), with time steps typically on the order of 10 nsec, and with running time typically on the order of a few hours on an IBM RS6000 workstation.

APPENDIX: VLASOV THEORY OF ION SOUND

In this section we show analytically that our quasineutral formulation, using the approximate form (4) for **E**, gives exactly the correct dispersion relation for linearized ion sound waves, including even the electron and ion Landau damping terms.

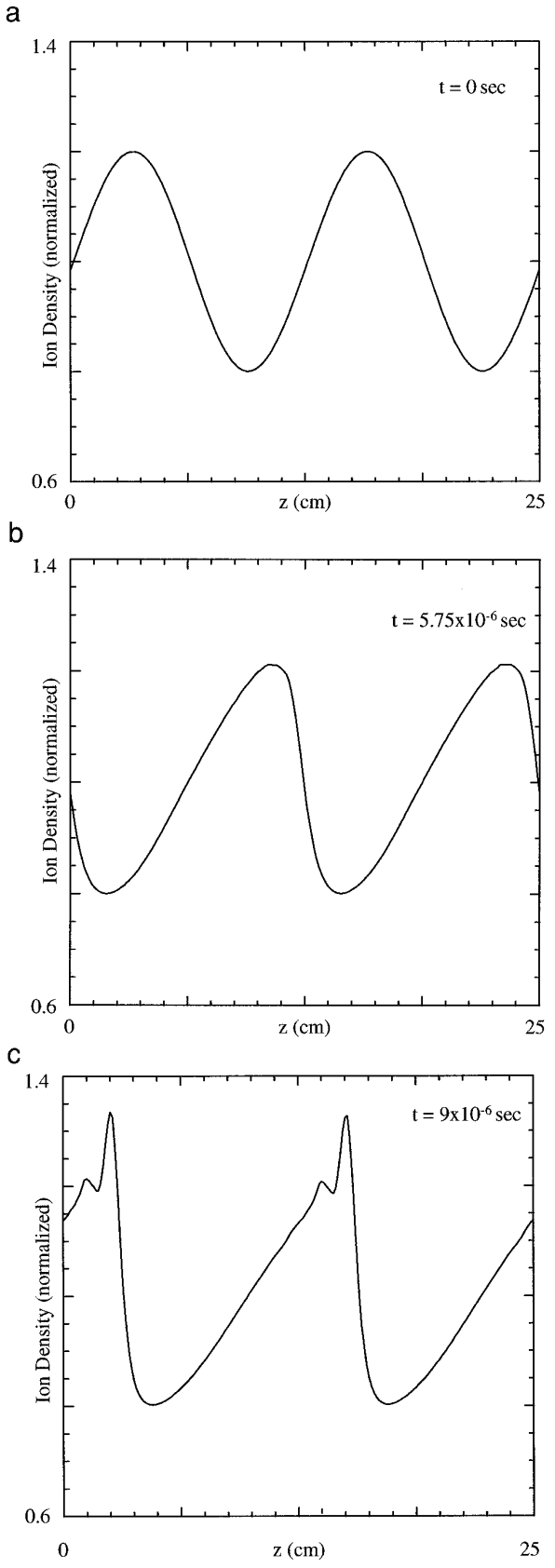

FIG. 5. Density profiles showing steeping of the traveling ion sound wave: (a) $t = 0$, (b) $t = 5.75$ μsec, (c) $t = 9.0$ μsec.

Review: Vlasov–Poisson Theory of Ion Sound

To clarify the issues involved, we begin with a brief review of the standard derivation of the ion sound dispersion relation from the linearized 1D Vlasov equation,

$$\frac{\partial f_\alpha}{\partial t} + v\frac{\partial f_\alpha}{\partial z} \mp \frac{n_0 eE}{m_\alpha}\frac{\partial F_{0\alpha}}{\partial v} = 0, \tag{A1}$$

with the upper sign for electrons and the lower sign for ions, and with the electric field E determined by Poisson's equation. Using a linearized normal mode representation for the perturbed part of the distribution function f_α, we find

$$f_{\alpha k}(v) = \pm\frac{in_0 eE}{m_\alpha}\frac{dF_{0\alpha}}{dv}\frac{1}{\omega - kv}, \tag{A2}$$

and the species densities $n_{\alpha k}$ are

$$n_{\alpha k} = \pm\frac{in_0 eE}{m_\alpha}\int \frac{dv\, F'_{0\alpha}(v)}{\omega - kv}. \tag{A3}$$

Inserting (A3) into Poisson's equation,

$$ikE_k = 4\pi(n_{ek} - n_{ik}), \tag{A4}$$

we obtain the dispersion relation,

$$0 = 1 - \frac{\omega_{pe}^2}{k^2}\int dv\,\frac{F'_{0e}(v)}{v - \omega/k} - \frac{\omega_{pi}^2}{k^2}\int dv\,\frac{F'_{0i}(v)}{v - \omega/k}, \tag{A5}$$

where causality indicates that the contours in Eqs. (A3) and (A5) go below the pole at $v = \omega/k$. The usual dispersion relation for ion sound can be obtained by making several approximations in Eq. (A5). First assume that the imaginary part of ω/k is small. Let u (which may be zero) be the relative electron–ion drift, and assume that $F_{0i}(v)$ is a symmetric function of v, but F_{0e} is a symmetric function of $w \equiv v - u$. Assume that $T_e \gg T_i$, $u \ll v_e$, and $v_i \ll \omega/k \ll v_e$. Then the first integral in Eq. (A5) can be treated by first extracting the contribution from the pole at $v = \omega/k$, and then expanding the remaining nonsingular integral under the assumption that $\omega/k \ll |w|$ and $u \ll |w|$ for nearly all electrons:

$$\int \frac{dv\, F'_{0e}(v)}{v - \omega/k} \cong -i\pi F'_{0e}\left(v = \frac{\omega}{k}\right) + \int \frac{dw\, F'_{0e}(w)}{w}\left[1 + \frac{\omega/k - u}{w} + \left(\frac{\omega/k - u}{w}\right)^2\right]. \tag{A6}$$

The second integral in Eq. (A5) can be treated by first extracting the contribution from the pole, and then expanding the remaining integral under the assumption that $\omega/k \gg |v|$ for nearly all ions:

$$\int \frac{dv\, F'_{0\mathrm{i}}(v)}{v-\omega/k} \cong -i\pi F'_{0\mathrm{i}}\left(\frac{\omega}{k}\right) - \frac{k}{\omega}$$
$$dv\, F'_{0\mathrm{i}}(v)\left(1+\frac{dv}{\omega}\right) = -i\pi F'_{0\mathrm{i}}\left(\frac{\omega}{k}\right) + \frac{k^2}{\omega^2}. \tag{A7}$$

Keeping only the leading term in the expansion (A6) gives the dispersion relation,

$$0 = 1 - \frac{\omega_{pe}^2}{k^2}\int \frac{dw\, F'_{0\mathrm{e}}}{w} - \frac{\omega_{pi}^2}{\omega^2} + \frac{k^2\omega_{pi}^2}{\omega^4}\int dv\, v^3 F'_{0\mathrm{i}} - \frac{i\pi}{k^2}\left[\omega_{pe}^2 F'_{0\mathrm{e}}\left(\frac{\omega}{k}\right) + \omega_{pi}^2 F'_{0\mathrm{i}}\left(\frac{\omega}{k}\right)\right]. \tag{A8}$$

In the case of Maxwellian velocity distributions, this reduces to the familiar form

$$\omega = \frac{kc_s}{(1+k^2\lambda_{\mathrm{D}}^2)^{1/2}} + \frac{i\pi}{2}\frac{kc_s}{(1+k^2\lambda_{\mathrm{D}}^2)^{3/2}}\left[\frac{T_{\mathrm{e}}}{m_{\mathrm{e}}}F'_{0\mathrm{e}}\left(\frac{\omega}{k}\right) + \frac{T_{\mathrm{e}}}{m_{\mathrm{i}}}F'_{0\mathrm{i}}\left(\frac{\omega}{k}\right)\right]. \tag{A9}$$

Quasineutral Derivation

In the quasineutral context, the electric field is determined by the linearized form of Eq. (4),

$$-eE_k = \frac{ikP_{\mathrm{e}k}}{n_0} + \frac{ikP_{0\mathrm{e}}}{n_0^2}(n_{\mathrm{i}k} - n_{\mathrm{e}k}), \tag{A10}$$

with

$$P_{\mathrm{e}k} = \int dv\, f_{\mathrm{e}k}(v) m_{\mathrm{e}} v^2 = in_0 eE\int \frac{dv\, F'_{0\mathrm{i}}(v)}{\omega - kv}. \tag{A11}$$

Using Eqs. (A3) and (A11) in (A10), we obtain the dispersion relation

$$0 = 1 + \int \frac{dv(v^2 - v_{\mathrm{e}}^2)F'_{0\mathrm{e}}}{v-\omega/k} - c_s^2\int \frac{dv\, F'_{0\mathrm{i}}}{v-\omega/k}. \tag{A12}$$

Equation (A12) looks different from Eq. (A5). Nevertheless, using the expansions (A6) and (A7) but keeping *all terms* shown in (A6) gives

$$0 = -\frac{\omega_{pe}^2}{k^2}\int \frac{dw\, F'_{0\mathrm{e}}}{w} - \frac{\omega_{pi}^2}{\omega^2} + \frac{k^2\omega_{pi}^2}{\omega^4}\int dv\, v^3 F'_{0\mathrm{i}} - \frac{i\pi}{k^2}\left[\omega_{pe}^2 F'_{0\mathrm{e}}\left(\frac{\omega}{k}\right) + \omega_{pi}^2 F'_{0\mathrm{i}}\left(\frac{\omega}{k}\right)\right]. \tag{A13}$$

Equation (A13) is identical to Eq. (A8), except for the absence of the first term on the RHS of (A8). This term is smaller than the other terms in (A8) by order $k^2\lambda_{\mathrm{D}}^2$, and thus disappears in the quasineutral limit $k\lambda_{\mathrm{D}} \to 0$.

REFERENCES

1. C. K. Birdsall and A. B. Langdon, *Plasma Physics via Computer Simulation* (Hilger, Bristol, 1991).
2. R. W. Hockney and J. W. Eastwood, *Computer Simulation Using Particles* (Hilger, Bristol, 1988).
3. T. Tajima, *Computational Plasma Physics* (Addison–Wesley, Reading, MA, 1989).
4. C. K. Birdsall and A. B. Langdon, *Plasma Physics via Computer Simulation* (Hilger, Bristol, 1991), p. 56.
5. J. Denavit, Time-filtering particle simulations with $\omega_p \Delta t \gg 1$, *J. Comput. Phys.* **42,** 337 (1981).
6. R. J. Mason, Implicit moment particle simulation of plasmas, *J. Comput. Phys.* **41,** 233 (1981).
7. A. Friedman, A. B. Langdon, and B. I. Cohen, A direct method for implicit particle-in-cell simulations, *Comments Plasma Phys. and Controlled Fusion* **6,** 25 (1981).
8. A. B. Langdon, B. I. Cohen, and A. Friedman, Direct implicit large time step particle simulations in plasmas, *J. Comput. Phys.* **51,** 107 (1983).
9. J. U. Brackbill and B. I. Cohen, eds., *Multiple Time Scales* (Academic Press, San Diego, 1985), Chaps. 8, 9, 11.
10. D. W. Hewett and D. J. Lawson, Solution of simultaneous partial differential equations using dynamic ADI: Solution of the streamlined Darwin field equations, *J. Comput. Phys.* **101,** 11 (1992).
11. C. K. Birdsall and A. B. Langdon, *Plasma Physics via Computer Simulation* (Hilger, Bristol, 1991), pp. 339–345.
12. F. F. Chen, *Introduction to Plasma Physics* (Plenum, New York, 1974), p. 66.
13. D. W. Hewett and C. W. Nielson, A multidimensional quasineutral plasma simulation model, *J. Comput. Phys.* **29,** 219 (1978).
14. J. K. Lee and C. K. Birdsall, Velocity space ring–plasma instability, magnetized, Part 1: Theory, *Phys. Fluids* **22,** 1306 (1979).
15. R. J. Mason, ''Hybrid and Collisional Implicit Plasma Simulation Models,'' in *Multiple Time Scales,* edited by J. M. Brackbill and B. I. Cohen (Academic Press, San Diego, 1985).
16. H. Okuda, J. M. Dawson, A. T. Lin, and C. C. Lin, Quasineutral particle simulation model with application to ion wave propagation, *Phys. Fluids* **21,** 476 (1978).
17. D. W. Hewett, A global method of solving electron–field equations in a zero-inertia-electron-hybrid plasma simulation code, *J. Comput. Phys.* **38,** 78 (1980).
18. A. G. Sgro and C. W. Nielson, Hybrid model studies of ion dynamics and magnetic diffusion during pinch implosions, *Phys. Fluids* **19,** 126 (1976).
19. J. A. Byers, B. I. Cohen, W. C. Condit, and J. N. Hanson, Hybrid simulation of quasi-neutral phenomena in a magnetized plasma, *J. Comput. Phys.* **27,** 363 (1978).
20. D. S. Harned, Quasi-neutral hybrid simulation of macroscopic plasma phenomena, *J. Comput. Phys.* **47,** 452 (1982).
21. A. Mankofsky, R. N. Sudan, and J. Denavit, Hybrid simulation of ion beams in background plasma. *J. Comput. Phys.* **70,** 89 (1987).
22. D. W. Hewett, Low-frequency electromagnetic (Darwin) applications in plasma simulation, *Comput. Phys. Commun.* **84,** 243 (1994).
23. C. K. Birdsall, Particle-in-cell charged particle simulations, plus Monte Carlo collisions with neutral atoms, PIC-MCC, *IEEE Trans. Plasma Sci.* **19,** 65 (1991).
24. R. W. Boswell and I. J. Morey, Self-consistent simulation of a parallel-plate RF discharge, *Appl. Phys. Lett.* **52,** 21 (1988).
25. D. Vender and R. W. Boswell, Numerical modeling of low pressure RF plasmas, *IEEE Trans. Plasma Sci.* **18,** 725 (1990).
26. M. Surendra, D. B. Graves, and I. J. Morey, Electron heating in low pressure RF glow discharges, *Appl. Phys. Lett.* **56,** 1022 (1990).
27. R. K. Porteus and D. B. Graves, Modeling and simulation of magnetically confined low pressure plasmas in two dimensions, *IEEE Trans. Plasma Sci.* **19,** 204 (1991).

28. D. B. Graves, H. Wu, and R. K. Porteus, Modeling and simulation of high density plasmas, *Japan, J. Appl. Phys.* **32,** 2999 (1993).
29. V. P. Gopinath and T. A. Grotjohn, Three-dimensional electromagnetic PIC model of a compact plasma source, *IEEE Trans. Plasma Sci.* **23,** 602 (1995).
30. V. Vahedi, C. K. Birdsall, M. A. Lieberman, G. DiPeso, and T. D. Rognlien, Capacitive RF discharges modeled by particle-in-cell Monte Carlo simulation. 1. Analysis of numerical techniques, *Plasma Sources Sci. Tech.* **2,** 261 (1993).
31. M. M. Turner and M. B. Hopkins, Anomalous sheath heating in low pressure RF discharges in nitrogen, *Phys. Rev. Lett.* **69,** 3511 (1992).
32. K. A. Ashtiani, J. L. Shohet, W. N. G. Hitchon, G.-H. Kim, and N. Hershkowitz, A two-dimensional particle-in-cell simulation of an electron-cyclotron-resonance etching tool, *J. Appl. Phys.* **78,** 2270 (1995).
33. M. Lampe, G. Joyce, and W. M. Manheimer, Quasineutral kinetic model of magnetized plasma discharges, in *Lectures in Plasma Physics and Technology,* edited by V. Stefan (La Jolla International School of Physics, 1998), in press.
34. W. M. Manheimer, M. Lampe, and G. Joyce, *Langevin Representation of Coulomb Collisions in PIC Simulations,* NRL Memorandum Report 6709-97-7894, 1997; *J. Comput. Phys.* **138** (1997).
35. M. Lampe, G. Joyce, W. M. Manheimer, and S. P. Slinker, *Quasineutral Particle Simulation of Magnetized Plasma Discharges: General Formalism and Application to ECR Discharges,* NRL Memorandum Report 6709-97-7960, 1997, *IEEE Trans. Plasma Science* 1988, in press.
36. C. K. Birdsall and A. B. Langdon, *Plasma Physics via Computer Simulation* (Hilger, Bristol, 1991), p. 437.
37. Landau and Lifschitz, *Fluid Mechanics* (Addison–Wesley, Reading, MA, 1959), pp. 366–386.
38. D. Montgomery, Evolution of a nonlinear ion acoustic wave, *Phys. Rev. Lett.* **19,** 1465 (1967).